Bioactive Materials 53 (2025) 706–717

Contents lists available at ScienceDirect

Bioactive Materials

journal homepage: www.keaipublishing.com/en/journals/bioactive-materials

Biocompatible liquid-infused titanium minimizes oral biofilm adhesion in flow chamber and 3D implant-tissue-biofilm *in vitro* models

Katharina Doll-Nikutta [a,b,*,1], Carina Mikolai [a,b,1], Nils Heine [a,b,1], Kestutis Kurselis [c], Elena Fadeeva [c], Nicolas Debener [d], Beate Legutko [e], Charlotte Kreuzkamp [a,b], Vannila Prasanthan [e], Janina Bahnemann [f,g], Boris N. Chichkov [c], Meike Stiesch [a,b]

[a] Department of Prosthetic Dentistry and Biomedical Materials Science, Hannover Medical School, Hannover, Germany
[b] Lower Saxony Center for Biomedical Engineering, Implant Research and Development (NIFE), Hannover, Germany
[c] Institute of Quantum Optics, Leibniz University Hannover, Hannover, Germany
[d] Institute of Technical Chemistry, Leibniz University Hannover, Hannover, Germany
[e] Institute of Production Engineering and Machine Tools, Leibniz University Hannover, Hannover, Germany
[f] Institute of Physics, University of Augsburg, Augsburg, Germany
[g] Centre for Advanced Analytics and Predictive Sciences (CAAPS), University of Augsburg, Augsburg, Germany

A B S T R A C T

Biomedical implants are susceptible to bacterial colonization, which can lead to challenging implant-associated infections. In particular, dental implant abutments – which are continuously exposed to bacteria within the oral cavity – stand to greatly benefit from strategies which inhibit the development of bacterial biofilms. Liquid-infused titanium surfaces have demonstrated excellent biofilm repellency, but to date have not been analyzed with substances suitable for medical device approval in terms of biocompatibility under conditions mimicking the environment of dental implant abutments. In this study, different medical-grade lubricants coated onto laser-structured titanium were screened for stability and water-repellency – with the results suggesting that unmodified structured titanium coated with silicone oil was the most promising combination of materials. When analyzing biofilm formation, the coated surfaces showed a statistically significant reduction in oral commensal *Streptococcus oralis* biofilms grown under static conditions as well as oral multispecies biofilms grown under salivation-resembling flow conditions. This biofilm-reducing effect was also observed when the coated surface interfaced with a 3D implant-tissue-oral-bacterial-biofilm (INTER$_b$ACT) *in vitro* model, which allows for the direct interaction of human tissue and oral multispecies biofilm at the implant interface. Importantly, this biofilm reduction was not due to toxicity of the coated surfaces, but is most likely attributable to inhibition of bacterial attachment. Additionally, the surfaces were not cytotoxic, without altering adjacent soft tissue or causing elevated pro-inflammatory cytokine secretion. These findings highlight the promise of biocompatible liquid-infused titanium surfaces as biofilm-repellent implant abutment modifications and provide the basis for further investigations in targeted pre-clinical studies.

1. Introduction

Titanium-based biomedical implants – like hip and knee endoprostheses, or dental implants – are well-known and long-established treatment options for the restoration of damaged body functions in modern medicine. However, due to their artificial nature (i.e., lacking any immune system in their own right), they are regrettably prone to bacterial colonization and development of implant-associated infections. This problem is especially severe for dental implants. To physiologically replace missing teeth, transmucosal positioning must unavoidably create permanent contact between the peri-implant tissue and the microbiome within the oral cavity. Out of the approximately 1.3 million dental implants that are inserted into patients within Germany every year, more than 25 % will develop an implant-associated infection five years after implantation [1,2]. Further complicating matters, the oral microbiome in question actually consists of a wide multitude of different

Peer review under the responsibility of editorial board of Bioactive Materials.

* Corresponding author. Hannover Medical School, Department of Prosthetic Dentistry and Biomedical Materials Science, Carl-Neuberg-Str. 1, 30625, Hannover, Germany.

E-mail addresses: nikutta.katharina@mh-hannover.de (K. Doll-Nikutta), Mikolai.Carina@mh-hannover.de (C. Mikolai), Heine.Nils@mh-hannover.de (N. Heine), Kurselis@lnqe.uni-hannover.de (K. Kurselis), Elena.Fadeeva@bakerhughes.com (E. Fadeeva), Debener@iftc.uni-hannover.de (N. Debener), Legutko@ifw.uni-hannover.de (B. Legutko), Charlotte.Kreuzkamp@web.de (C. Kreuzkamp), Prasanthan@ifw.uni-hannover.de (V. Prasanthan), Janina.Bahnemann@uni-a.de (J. Bahnemann), Chichkov@iqo.uni-hanover.de (B.N. Chichkov), Stiesch.Meike@mh-hannover.de (M. Stiesch).

[1] Equally contributing authors.

https://doi.org/10.1016/j.bioactmat.2025.07.048
Received 31 January 2025; Received in revised form 25 July 2025; Accepted 28 July 2025
Available online 1 August 2025

bacterial species that adhere to solid surfaces and grow into highly structured biofilms, featuring specific ecological niches and metabolic support networks as well as a protective matrix of extracellular polymeric substances [3,4]. These biofilms frequently show increased tolerance towards antibacterial substances and an ability to hitchhike the immune system via overall reduced cell division rate, altered metabolic processes, and the fact that the matrix can function as a physical diffusion barrier [3,5]. This bacterial presence activates the innate immune system and causes a local inflammatory reaction which is characterized by an increase in pro-inflammatory cytokines and the invasion of innate immune cells. Oral pathogens embedded inside the biofilm can use this to their advantage and modify the immune response to maintain pro-inflammatory conditions while evading their own clearance by invasion into the tissue [6]. Consequently, the prolonged inflammatory conditions can cause a disruption of the human tissue down to the alveolar bone – ultimately leading, in severe cases, to implant loss.

One possible solution to reduce the number of implant-associated infections lies in the prevention of bacterial biofilm development and its consequences via the inhibition of the first step of biofilm formation: the bacterial surface attachment. Modern dental implants consist of three parts: the osseointegrated implant screw, the transmucosal abutment and the orally exposed crown. Whereas the implant screw is mechanically drilled into the supporting bone and requires a stable attachment of osteoblast and connective tissue cells, the abutment is placed into a prepared mucosal passage with significantly less mechanical forces. Also, depending on the exact implant position, the abutment is not directly tissue integrated and protrudes into the oral cavity. Due to this position, the abutment can be considered the starting point for biofilm formation, subsequent apical expansion and infection onset. Therefore, reducing bacterial attachment to the dental implant abutment could significantly contribute to reduce implant-associated infections.

A particularly promising antiadhesive surface functionalization is the concept of liquid-infused surfaces (LIS). This biomimetic approach is based on the trapping mechanism of carnivorous Nepenthes pitcher plants: A structured surface is covered by a lubricant that is immiscible to the surrounding, and, due to matching physicochemical characteristics, energetically prefers to spread on the surface [7]. In our previous work, we have developed a LIS modification of the implant material titanium by (I) physically structuring the surface using ultra-short pulsed laser ablation, (II) adapting the physicochemical surface characteristics with a fluoropolymer, and (III) infusing the surface with a medium viscous perfluoropolyether [8]. The resulting titanium LIS displayed a very low droplet sliding angle (contact angle hysteresis), remained stable under physiological flow conditions, and exhibited strong biofilm-repellency towards an oral multispecies biofilm *in vitro* [8,9]. Importantly, the latter effect was not due to any toxicity of the LIS components, but rather solely to a significant reduction of bacterial adhesion forces leading to their removal under salivary flow conditions [8,9].

However, even though the fluoropolymer components used showed no cytotoxicity towards human cells at low concentration [8], they lack medical device approval. Additionally, previous experiments were done in simplified *in vitro* settings which don't fully capture the specific environmental conditions of dental implant abutments, featuring side-to-side contact between abutment material, connective tissue, and bacterial cells. Recently, titanium LIS made up from certified biocompatible lubricants that are suitable for medical products (like chitosan and silicone) have been reported [10,11]. They were assessed under experimental *in vitro* conditions for orthopedic and marine applications. Yet LIS tested under physiological conditions of biomedical devices remains limited to silicone catheter tubes, basic research on the immune reaction to subcutaneously placed LIS, and a direct modification of rabbit teeth [12–16]. To date, no analysis of biocompatible titanium LIS under physiological conditions relevant to dental implant abutments has yet been conducted.

Accordingly, the dual aims of the present study are (I) to develop a biocompatible, medical-grade LIS modification on titanium that maintains stability and biofilm repellency under complex physiologically relevant conditions mimicking the environment of dental implant abutments and (II) to analyze how this modification influences the interaction of human connective tissue and oral multispecies biofilm next to the abutment surface. For this purpose, promising biocompatible titanium LIS combinations that have been identified by physical characterization were subjected to two physiological *in vitro* models: the Hannoverian oral multispecies biofilm implant flow chamber (HOBIC) model, which reproduces multispecies biofilm formation under salivary flow conditions [17], and a 3D implant-mucosal tissue-oral biofilm co-culture INTER$_b$ACT model that allows for the analysis of oral bacteria-cell interactions at the implant material interface [18]. The results of this work constitute a promising titanium LIS modification suitable for medical devices that can be transferred to targeted pre-clinical studies.

2. Materials and methods

2.1. Preparation of liquid-infused titanium

For initial material and biological characterization, titanium grade 4 discs (12 mm or 3 mm in diameter, 1.2 mm in height) were used and structured via femtosecond pulsed laser ablation (Femtopower Compact Pro, Femtolasers Production GmbH, Spectra Physics, Vienna, Austria) as described previously [8]. To generate spike structures, the scanning speed along its linear polarization direction (x-direction) was 800 µm/s with a translational step in y-direction of 15 µm and a laser ablation fluence of 8 J/cm^2. For ripple structures, the scanning speed in x-direction was 1000 µm/s, the translation step in y-direction was 14 µm and the laser ablation fluence was 0.5 J/cm^2. For experiments in the 3D implant-tissue-oral bacterial biofilm model (INTER$_b$ACT), titanium grade 4 cylinders (3 mm in diameter, 2.7 mm in height) were used. One half horizontally was laser ablation structured with similar spikes using the Spitfire Pro 35F-XP laser system (40 fs pulses, 800 nm wave length, 1 kHz repetition rate, Newport Spectra-Physics GmbH, Darmstadt, Germany) and a biconvex lens with a focal length of 125 mm for focusing. Structuring was done at an average power of 100 mW (which corresponds to a pulse energy of 100 µJ) with a scanning speed in x-direction of 1000 µm/s and a translational step in y-direction of 15 µm. Control samples and spike structures were analyzed for their surface topography using an optical measuring device (DuoVario, Confovis GmbH, Jena, Germany) with a 20x objective and a measuring field of 630× 630 µm^2, and the µsoft analysis premium 8.2 software (Digital Surf, Besancon, France) for evaluation. 3 samples of each type were analyzed at 3 different spots (N = 9) for the surface characteristics S10z, Sa, and Sz. By this, uniform surface topography could be ensured (Appendix Figure A1). To generate LIS (Fig. 1A), the surfaces were (1) sterilized by autoclaving, (2) optionally functionalized by surface covering drip on of volatile liquids (Table 1) and then (3) coated with 20 µl (12 mm discs), 2 µl (3 mm discs), or 3 µl (3 mm cylinders) of viscous lubricants (Table 1). Liquid-infused samples were tilted once to remove excess lubricant and then UV sterilized for 20 min prior to biological experiments. Polished (R_a = 0.3 µm [19]), autoclaved titanium grade 4 discs and cylinders of similar size served as control samples. LIS were always used directly after preparation and not stored.

2.2. Contact angle and lubricant stability measurement

Static contact angle on the disc shaped LIS was measured using 12 mm discs and a commercial contact angle measuring device (OCA 40, DataPhysics Instrumtents GmbH, Filderstadt, Germany) as well as a water droplet of 20 µl. By tilting the device, contact angle hysteresis could be determined vis-á-vis the difference between the retracting and

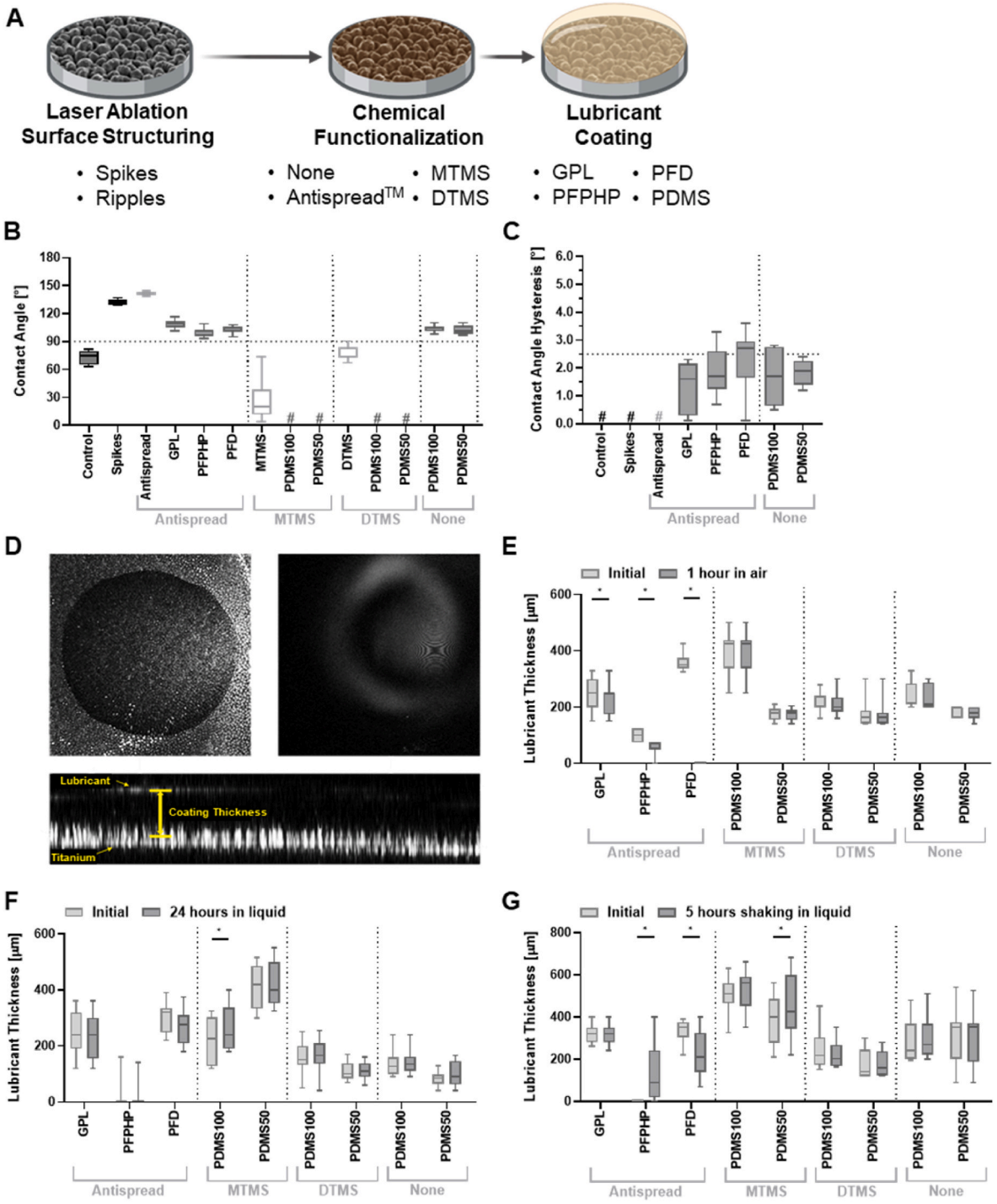

Fig. 1. Characteristics of liquid-infused titanium with spike structure, different functionalization and lubricant coating. (A) Schematics showing LIS generation from different components in this study. (B) Tukey box plots of static water contact angles and (C) water contact angle hysteresis of different liquid-infused titanium compositions. # indicates surfaces, where no measurement was possible due to water creeping below the lubricant (contact angle) or droplet sticking (contact angle hysteresis). MTMS and DTMS functionalized spikes were excluded from contact angle hysteresis due to this reason. Horizontally dotted lines indicate relevant thresholds. (D) CLSM reflection images of liquid-infused titanium at the titanium level (left) and at the highest point of the lubricant (right) with resulting lubricant thickness quantification (bottom). (E) Tukey box plots of lubricant thickness before and after incubation in ambient air, (F) in phosphate buffered saline, and (G) in phosphate buffered saline with shaking of different liquid-infused titanium compositions. * indicates statistically significant differences with $p \leq 0.05$ to the control or as indicated.

advancing contact angle just before the droplet started sliding. Water contact angle and contact angle hysteresis on PDMS100 were also measured after incubating LIS in air for 7 days at 37 °C. Lubricant stability measurement after 1 h in ambient air, after 24 h in liquid (phosphate buffered saline, PBS, Biochrome GmbH, Berlin, Germany) and after 5 h shaking in liquid with 500 rpm was determined via reference to lubricant thickness measurement using confocal laser scanning microscopy (CLSM, Leica SP8, Leica Microsystems, Mannheim, Germany) with a 488 nm laser line, detection in the reflection mode (485–490 nm), 100-fold magnification and a z-step size of 25 µm. Additionally, stability

Table 1
Substances used for LIS generation.

Abbreviation	Substance	Application
Antispread	Fluoropolymer Antispread™ E2/30 FE60 (Dr. Tilwich GmbH Werner Stehr, Horb-Ahldorf, Germany)	Surface functionalization
MTMS	Methyltrimethoxysilane (Sigma-Aldrich, St. Louis, MO, USA)	Surface functionalization
DTMS	Decyltrimethoxysilane (Sigma-Aldrich)	Surface functionalization
GPL	Perfluoropolyether Krytox GPL 104 (DuPont de Nemours, Neu-Isenburg, Germany)	Surface coating
PFPHP	Perfluoroperhydrophenanthrene (Sigma-Aldrich)	Surface coating
PFD	Perfluorodecalin (Sigma-Aldrich)	Surface coating
PDMS50	Polydimethylsiloxane with viscosity of 50 cSt (Sigma-Aldrich)	Surface coating
PDMS100	Polydimethylsiloxane with viscosity of 100 cSt (Sigma-Aldrich)	Surface coating

of PDMS100 LIS was measured over the course of 7 days in a flow chamber setup with a constant flow of PBS at 100 μL/min with daily flushes of 1500 μL/min for 1 min. From the resulting 3D images, the layer with the strongest titanium reflection and the last layer with visible lubricant were selected and the coating thickness was determined (Fig. 1D) using the Imaris x64 8.4.1 software package (BitPlane AG, Zürich, Switzerland). Contact angles and lubricant stability were analyzed in N = 9 replicates. Following D'Agostino & Pearson's normality test, statistical differences were calculated for static contact angles using ordinary one-way ANOVA with Dunnett's test for multiple comparisons to a single group or with Tukey's test for multiple comparisons among several groups. For contact angle hysteresis, statistical differences were calculated using Kruskal-Wallis test with Dunn's multiple comparison test and for lubricant stability, two-way repeated measures ANOVA with uncorrected Fisher's LSD test for multiple comparisons was applied.

2.3. Antibacterial effect of LIS components

To analyze antibacterial effects of the LIS components, the oral commensal bacterium *Streptococcus oralis* (ATCC 9811, American Type Culture Collection, Manassas, VA, USA) was used. After pre-culture in tryptic soy broth (TSB, Oxoid Limited, Hampshire, UK) supplemented with 10 % yeast extract (TSBy, Carl Roth GmbH & Co. KG) for 20 h shaking at 37 °C in ambient air, the bacteria were adjusted to an optical density at 600 nm (OD_{600}) of 0.01 in TSBy. They were incubated with different concentrations of functionalization chemicals, lubricants, or sterile water as growth control under rigorous shaking at 500 rpm to enforce contact between lubricants and bacteria. After cultivation for 24 h at 37 °C in ambient air, bacterial viability was quantified using the BacTiter-Glo assay (Promega, Mannheim, Germany) according to the manufacturer's protocol and then normalized to the water control. Antibacterial effects were analyzed in N = 9 replicates and statistical differences between components and water control at each concentration were calculated using Two-way ANOVA with Dunnett's multiple comparison test.

2.4. Static biofilm growth of Streptococcus oralis

Growth of *S. oralis* (ATCC 9811) monospecies biofilms was analyzed on LIS prepared on 3 mm discs. Pre-cultures were grown as described before, and then diluted to an OD_{600} of 0.1 in TSBy with addition of 50 mM glucose (Carl Roth GmbH & Co. KG). Titanium discs with LIS coating were placed into 6-well plates (three technical replicates within one well) and submerged with the bacterial suspension. After cultivation for 24 h at 37 °C in ambient air and washing twice with PBS, biofilm growth and membrane integrity-based viability was analyzed via fluorescence staining and confocal microscopy (described below). Additionally, growth of *S. oralis* monospecies biofilms on LIS was analyzed after cultivation for 7 days. For this, half-structured 12 mm discs were used, resulting in one control surface and one LIS per disc, with one disc per well in 6-well plates. Every other day, half of the medium in each well was replaced with fresh TSBy with 50 mM glucose. Experiments were done in N = 9 replicates. Biofilm volume data were tested for Gaussian distribution using the D'Agostino & Pearson normality test and analyzed for statistical differences by Kruskal-Wallis test with Dunn's multiple comparison correction. Distribution of membrane integrity was assessed using Two-way ANOVA with Tukey's multiple comparison test.

2.5. Flow chamber growth of an oral multispecies biofilm

The Hannoverian Oral Multispecies Biofilm Implant Flow Chamber (HOBIC) model was used to analyze multispecies biofilm growth on LIS prepared on 12 mm discs as described previously [9,17]. In brief, *S. oralis* (ATCC 9811), *Actinomyces naeslundii* (DSM 43013, German Collection of Microorganisms and Cell Cultures (DSMZ), Braunschweig, Germany), *Veillonella dispar* (DSM 20735, DSMZ) and *Porphyromonas gingivalis* (DSM 20709, DSMZ) were pre-cultured in brain heart infusion (BHI, Oxoid Limited) supplemented with 10 μL/mL vitamin K (Oxoid Limited) for 18 h at 37 °C under anaerobic conditions (air-tight containment with Thermo Scientific™ Oxoid™ AnaeroGen™ 2.5 L bags (Fisher Scientific GmbH, Schwerte, Germany)). Pre-cultures were adjusted to an OD_{600} of 0.1 (corresponding to 2×10^{13} CFU/mL for *S. oralis*, 2×10^{10} CFU/mL for *A. naeslundii*, 5×10^{8} CFU/mL for *V. dispar*, and 1×10^{9} CFU/mL for *P. gingivalis*), mixed in equal volumes, and added to 2 L of the same medium in the bioreactor of the HOBIC model. The system was then run for 24 h with 100 μL/min at 37 °C under anaerobic conditions (attachment of N_2 overpressure balloon). Afterwards, biofilms were pulsed washed with PBS as described previously [9], fluorescence stained, and finally analyzed by confocal microscopy (described below). Experiments were done in N = 3 replicates and biofilm volume and membrane integrity-based viability were analyzed as described for *S. oralis* monospecies biofilms. As more sophisticated methods for quantitative or qualitative species identification were not applicable for LIS samples, additionally, bacteria shapes and biofilm structures in the resulting CLSM images were qualitatively analyzed to compare biofilms on PDMS100-LIS and titanium.

2.6. Cytotoxic effect of LIS components

The potential cytotoxic effect of the LIS components was analyzed using oral keratinocytes (OKF6/TERT-2) [20], cultivated in Keratinocyte Serum-Free Medium (KerSFM; 10725-018, Gibco Life Technologies) supplemented with 0.3 mM $CaCl_2$, 0.2 mg/mL epidermal growth factor (Gibco™, Fisher Scientific GmbH), 25 μg/mL bovine pituitary extract (Fisher Scientific GmbH), 100 U/mL penicillin, and 100 μg/mL streptomycin (both Sigma Aldrich), and human gingival fibroblasts (HGF; 121 0412, Provitro, Berlin, Germany), cultured in Dulbecco's Modified Eagle's Medium (DMEM; P04-04500, PAN-Biotech GmbH, Germany) supplemented with 10 % fetal bovine serum (FBS; P30-3309, PAN-Biotech GmbH), 100 U/mL penicillin, and 100 μg/mL streptomycin. OKF6/TERT-2 or HGFs were seeded into 96-Well plates with 1500 cells/well or 3000 cells/well, respectively. After incubation for 24 h at 37 °C in humidified atmosphere (5 % CO_2), fresh medium containing the different LIS components (or alternately sterile water as growth control) was added and incubated another 24 h. Cellular metabolic activity was quantified using the CellTiter-Blue Cell Viability Assay (Promega, Mannheim, Germany) according to the manufacturer's protocol. Cytotoxicity was analyzed in N = 9 replicates, and statistical differences between components and water control at each concentration were calculated using Two-way ANOVA with Dunnett's multiple comparison test.

2.7. LIS integration and biofilm co-culture in the INTER$_b$ACT model

The 3D-implant-tissue-oral bacterial biofilm model (INTER$_b$ACT) was assembled as described previously in detail [18,21]. For the construction of the organotypic peri-implant mucosa, HGFs (4×10^5 cells/model) were embedded in a collagen hydrogel (bovine type-I collagen (3 mg/mL, PureCol®, 5005-100 ML, Advanced BioMatrix, Carlsbad, CA, USA), FBS, L-glutamine (G7513, Sigma-Aldrich), 10x DMEM (P03-01510, Pan-Biotech), reconstitution buffer (2 mg/mL sodium bicarbonate, 2 mM HEPES, and 0.0062 N NaOH)), seeded into culture inserts (3414, Corning B.V. Life Sciences, Berlin, Germany) and cultivated at 37 °C in 5 % CO_2 humidified atmosphere for five days. Cylindric PDSM100-LIS and control samples were colonized upside down with HGFs (1×10^6 cells/mL) at 37 °C in 5 % CO_2 humidified atmosphere for five days before being inserted into the HGF-containing hydrogel with the modified part upwards. After 3 days, OKF6/TERT-2 (1×10^6 cells/model) were seeded on top of the implant-integrated HGF-hydrogel. Following 48 h of cultivation, models were raised to an air-liquid interface and were cultivated with Airlift (AL)-medium (3:1 DMEM (P04-03591, Pan-Biotech) and Ham's F-12 (P04-14559, Pan-Biotech), 5 μg/mL insulin, 0.4 μg/mL hydrocortisone, 2×10^{-11} M 5 triiodo-L-thyronine, 1.8×10^{-5} M adenine, 5 μg/mL transferrin, 10^{-10} M cholera toxin, 2 mM L-glutamine, 10 % v/v FBS, 1 % v/v penicillin/streptomycin (all supplements Sigma Aldrich)) at 37 °C in 5 % CO_2 humidified atmosphere for further 15 days to simulate epithelial differentiation and stratification. The multispecies biofilms were formed as described previously (Mikolai et al., 2020, Kommerein et al., 2017). Briefly, the four species *S. oralis*, *A. naeslundii*, *V. dispar* and *P. gingivalis* were separately pre-cultured as described above. Pre-cultures were OD_{600}-adjusted in BHI/vitamin K and mixed equally to achieve a final OD_{600} of 0.01 for each species. The bacterial suspension was seeded on glass cover slips (10 mm in diameter, thickness 1, Thermo Scientific Menzel, Fisher Scientific GmbH) and allowed for biofilm formation for 48 h at 37 °C under anaerobic conditions. For co-culture assembly of the INTER$_b$ACT model, the organotypic peri-implant mucosa and the multispecies biofilm were washed once with PBS. The LIS implants were re-coated with 3 μl PDMS100 and the biofilm cover slips were placed on top of integrated implant (control and LIS) with the biofilm side facing towards implant and mucosa. Co-culture was conducted in co-culture medium (AL-medium without penicillin/streptomycin, supplemented with 10 % v/v BHI/vitamin K) for 48 h at 37 °C in humidified % CO_2 atmosphere. After 24 h, the medium outside of culture insert was replaced once.

2.8. Live/dead fluorescence staining, confocal laser scanning microscopy and digital image analysis

The LIVE/DEAD®*Bac*Light™ Bacterial Viability Kit (Fisher Scientific GmbH) was applied with both dyes (Syto9 and propidium iodide) diluted 1:2000 in PBS for 15 min to static biofilms, for 20 min with 250 μL/min in the HOBIC model and for 30 min to the INTER$_b$ACT model. Afterwards, samples were fixed with 2.5 % glutardialdehyde in PBS using the same conditions – but for static biofilms and the INTER$_b$ACT model at 4 °C – before samples were covered with PBS for microscopy. Implants of the INTER$_b$ACT model were detached from the mucosa before analysis. Using a confocal laser scanning microscope (SP8, Leica Microsystems, Mannheim, Germany), Syto9 was excited with a 488 nm laser and emission was detected at 500–540 nm, and propidium iodide was excited with a 552 nm laser and emission was detected at 650–700 nm. In parallel, surface reflection was recorded at 485–490 nm. From each sample, five three-dimensional image series (four in the case of the INTER$_b$ACT model) were taken at standardized positions with a magnification of 400-fold corresponding to an image size of 295 × 295 μm^2. Quantification of biofilm volume and membrane integrity-based vitality distribution was accomplished using the Imaris x64 8.4.1 software package (Bitplane AG, Zurich, Switzerland) using the surface wizard. For images of the INTER$_b$ACT model, the z-stacks of each image were converted into a single image by maximum intensity projection and quantified for surface coverage using the ImageJ software [22] and cell/bacteria surface coverage distribution using the graphical user interface of Cellpose 2.0 in a human-in-the-loop approach [23]. For the latter, after manually drawing the regions of interest for the first image, a new Cellpose model was trained to segment single bacteria and microcolonies (Appendix Figure A5). This model was then refined through a process of retraining and manual correction – a procedure which was repeated for the first 13 images. Subsequently, a new model was trained based on these 13 annotated images, with a learning rate of 0.1 and 1000 training epochs. Following the automatic segmentation of the remaining images with this model, undetected bacteria as well as larger biofilm patches were added manually. The bacterial surface coverage of each image was then calculated by dividing the number of nonzero elements in the final mask (= pixels belonging to bacteria) by the total number of pixels within the image.

2.9. Enzyme-linked immunosorbent assays

To quantify cytokine and chemokine secretion, supernatants of the INTER$_b$ACT models after finishing tissue differentiation (integration group) and after biofilm coculture (coculture group) were centrifuged to remove cell debris and then analyzed using commercially available enzyme-linked immunosorbent assay (ELISA) kits (human IL-1β, human IL-6, human TNFα all ABTS ELISA Development Kit, PeproTech GmbH, Hamburg, Germany; human CCL20 ELISA MAX™ Deluxe Set, BioLegend Inc, San Diego, CA, USA) according to the manufacturer's protocols. Samples were analyzed in N = 6 and N = 8 replicates for integration and coculture, respectively. After interpolation to the standard curves (Appendix Figure A6A), data were analyzed for Gaussian distribution using the D'Agostino & Pearson normality test, and statistical differences between control and LIS samples were tested using the unpaired *t*-test. Cytokine levels between integration and coculture were compared using Two-way ANOVA with Šídák's multiple comparison test.

2.10. Histology of the INTER$_b$ACT model

Histological analysis was done by MORPHISTO GmbH (Offenbach am Main, Germany) as described previously [21]. In brief, tissues were fixed in 4 % buffered formalin solution and embedded in Technovit 9100. After being cut and grinded to slides of approx. 35 μm thickness, tissues were stained according to Elastica van Gieson.

2.11. Statistical analysis

Data presentation and statistical analysis were accomplished using the GraphPad Prism software v10.4.1 (GraphPad Software, Boston, MA, USA). The number of replicates and performed statistical tests are stated in the respective experimental sections. Family-wise significance level was always set to $\alpha = 0.05$.

3. Results

3.1. Water repellency and high stability of silicone-infused titanium

To develop medical device-suitable liquid-infused titanium surfaces, several different combinations of structures, functionalization and lubricant coatings were tested (Fig. 1A). Aside from the medical-grade lubricants perfluoroperhydrophenanthrene (PFPHP), perfluorodecalin (PFD), and polydimethylsiloxane (with two viscosities, PDMS50 and PDMS100), the perfluoropolyether GPL was also included as a control lubricant with known LIS-forming ability [8]. Since stable wetting of the surface by the lubricant is a central aspect of the LIS principle [7], this was initially tested by static water contact angle measurement (Fig. 1B–Appendix Figure A2A, B). The changes in contact angle

compared to the uncoated spike surfaces indicated a stable immersion of the underlying structure by the coated lubricants. Similar results were obtained on ripple structures coated with PFPHP and PFD (Appendix Figure A2B). In contrast, after MTMS and DTMS functionalization of spikes (which made them more hydrophilic), no contact angles could be measured because the water droplet crawled below the lubricant. Thus, no sufficient lubricant coating could be achieved for this combination. Another characteristic parameter for successful LIS generation is a strong liquid repellency indicated by very low water contact angle hysteresis of $< 2.5°$ [7]. This requirement could only be met for spikes functionalized with Antispread and coated with GPL, PFPHP, and PFD as well as unfunctionalized spikes coated with PDMS50 and PDMS100 (Fig. 1C). For all other combinations, the water droplets stuck to the surface and did not allow for contact angle hysteresis measurement. Additionally, for PDMS100 coated onto unfunctionalized spikes, water contact angle and contact angle hysteresis were measured after 7 days of incubation at 37 °C, and were not significantly different to the values measured directly after LIS preparation (Appendix Figure A3B, C).

To further analyze LIS stability over time, lubricant thickness of the different combinations was measured via confocal reflection microscopy (Fig. 1D–Appendix Figure A2C). In general, the lubricant thickness varied between the different combinations, with MTMS functionalized spikes coated with PDMS showing the thickest coating of up to 400 µm and coatings with PFPHP showing the thinnest layer of approx. 100 µm. After one hour at ambient air, statistically significant thickness reductions were observed for GPL (by approx. 5 %), PFPHP (by approx. 50 %), and PFD (by approx. 100 %) coatings, independently of the underlying surface (Fig. 1E). The thickness of all PDMS coatings did not change when they were incubated in air. When analyzing lubricant stability after 24 h of incubation in physiological liquid (PBS), PFPHP and PFD showed the most noticeable changes (Fig. 1F). For PFPHP, no lubricant could be measured on spike structures, and very little lubricant

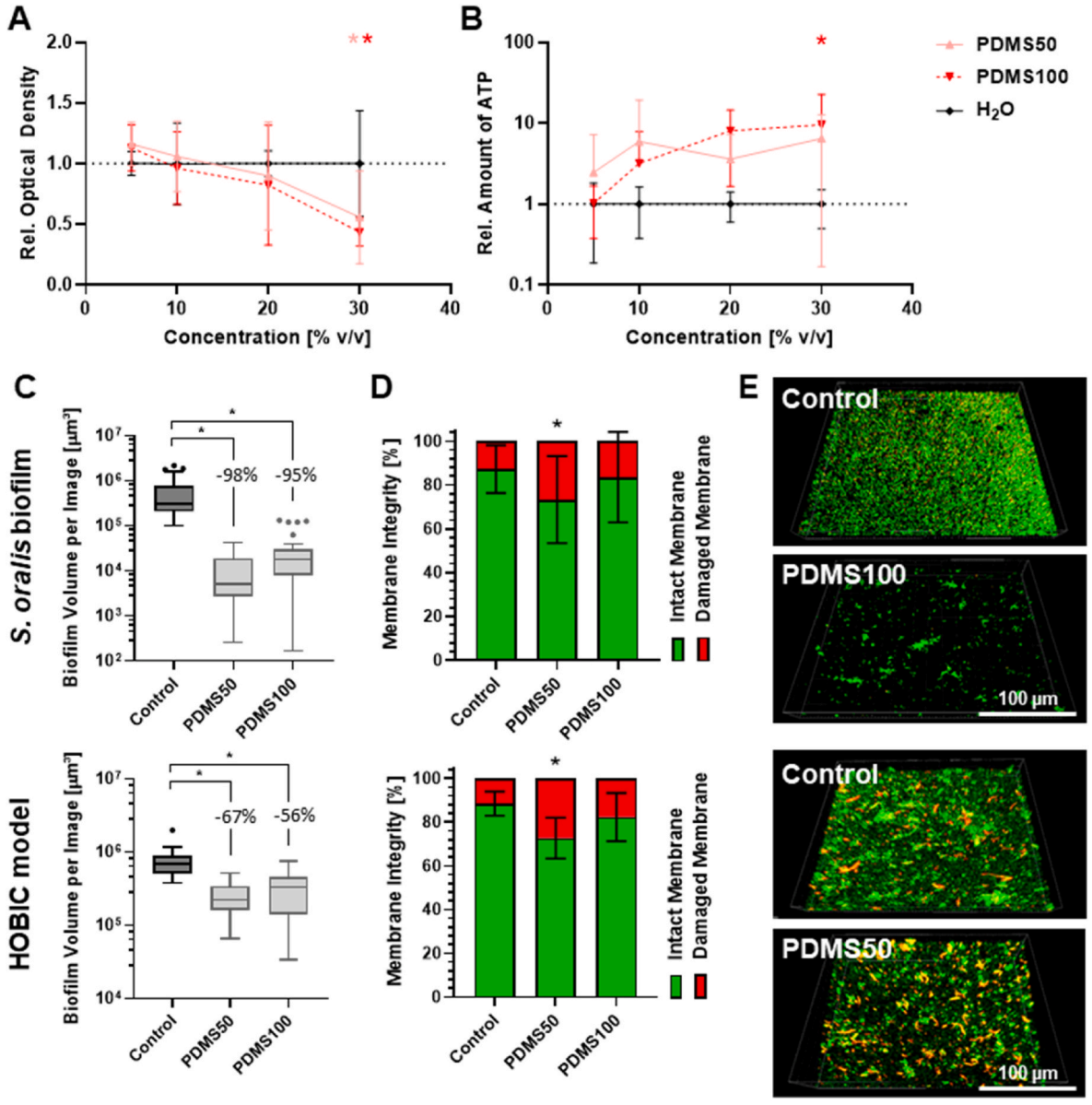

Fig. 2. Biofilm-repellent properties of spike structured titanium with silicone coating. (A) Mean ± standard deviation of planktonic S. oralis growth and (B) metabolic activity after 24 h incubation with different LIS components. * indicate statistically significant differences to the respective water control with $p \leq 0.05$. (C–E) *S. oralis* static monospecies biofilm growth and oral multispecies biofilm growth in the HOBIC model showing each (C) Tukey boxplots of biofilm volume, (D) mean ± standard deviation of membrane-based biofilm viability, and (E) representative 3D CLSM image reconstructions. Viable cells are depicted in green; damaged cells are depicted in yellow/red. * indicates statistically significant differences to the control with $p \leq 0.05$.

could be measured on ripples. For PFD, lubricant thickness stayed stable on spike structures but showed great variability on ripples, indicating a lack of stable surface coating. Interestingly, PDMS100 on MTMS functionalized spikes exhibited a significant increase in lubricant thickness by approx. 20 %. Most probably, this is due to lubricant contraction towards the center of the surface, which can also be considered a form of instability of the coating. All other combinations showed stable lubricant thickness – albeit an overall thinner coating thickness when compared to incubation in air. Finally, coating stability was tested in physiological liquid with continuous shaking at 500 rpm (Fig. 1G). The results are similar to those without shaking, with PFPHP and PFD showing clearly unstable surface coatings and PDMS100 showing centralization on MTMS functionalized spikes. All other combinations maintained a stable lubricant coating. Additionally, PDMS100-LIS on uncoated spikes were tested for their stability for 7 days under constant flow in a flow chamber setup. After a certain, non-significant initial drop of lubricant thickness the thickness remained constant over the course of 7 days (Appendix Figure A3A).

Taking all of these measurements into account, we determined that liquid-repelling LIS using medical-grade lubricants could be generated when coating PDMS50 and PDMS100 lubricants on spike structured titanium without further surface functionalization. Therefore, this combination became the focus and subject of our further biological investigations.

3.2. Biofilm-repellent properties of silicone-infused titanium

Before assessing the LIS' biofilm-repellency, potential antibacterial effects of the individual components were tested by incubating them with planktonic *S. oralis*. Low concentrations of LIS components did not have adverse effects on bacterial growth and viability (Fig. 2A and B). With increasing concentration, however, bacterial growth by means of optical density was found to be significantly reduced (Fig. 2A). In parallel, metabolic activity (quantified as amount of ATP produced) increased, which supports the observed stress reaction (Fig. 2B). In the next step, *S. oralis* monospecies biofilms were grown on the different LIS under static conditions (Fig. 2C–E). On both combinations, biofilm volume was significantly reduced by more than 95 % when compared to the control (see Fig. 2C–E). In parallel, membrane integrity as marker of biofilm viability, which was 87 % on the control surfaces, was only reduced on PDMS50 to 73 % (Fig. 2D). To test whether the LIS retain their biofilm-repelling effect over longer periods of time, *S. oralis* was also incubated with PDMS100-LIS and control titanium for 7 days, which resulted in a reduction of biofilm on LIS by 87 % compared to the control (Appendix Figure A3D, E). Since biofilms within the oral cavity are composed from a multitude of different bacterial species and are exposed to constant saliva flow, LIS were also analyzed in the established HOBIC model, containing a commensal four-species biofilm grown under flow conditions [17]. Once again, biofilm volume significantly decreased on all LIS combinations (Fig. 2C–E). However, compared to static *S. oralis* monospecies biofilms, the extent of this decrease was comparatively lower – with a reduction of 65 %, and 55 % on PDMS50 and PDMS100 coated surfaces, respectively. To qualitatively check whether the composition of multispecies biofilms on LIS is different from biofilms grown on titanium, which would indicate genus- or species-level differences in functionality, bacteria shapes and biofilm structures visible in live/dead-stained biofilms on PDMS100-LIS and titanium were compared (Appendix Figure A4). On both surfaces, *S. oralis* could be identified by long chains of small cocci in abundant amounts. Larger cocci, alone or in clusters, indicated the presence of *V. dispar* on both surfaces in similar proportions. Some small clusters of long, rod-shaped bacteria, which can be attributed to *A. naeslundii,* could also be spotted on both surfaces. Due to its similar shape and low abundance, *P. gingivalis*, cannot be identified by this method [17]. Biofilm structures were also similar between both surfaces, with several small-to medium-sized bacteria clusters being present. The amount of viable bacteria significantly decreased on PDMS50 coated surfaces to 73 %, whereas biofilms on all other surfaces showed 82–90 % viable cells (Fig. 2D).

3.3. Intact soft tissue in direct contact to silicone-infused titanium

Prior to the analysis of tissue reaction when being put site-to-site with the titanium LIS, the individual components were tested for cytotoxic effects and adhesion of monolayers of oral keratinocytes (Fig. 3A, Appendix Figure A7) and gingival fibroblasts (Fig. 3B–Appendix Figure A7). Metabolic activity of epithelial cells was found to be significantly reduced only at the lowest concentration of 5 % PDMS50 and PDMS100, but it still remained above the cytotoxic threshold of 0.8. For fibroblasts, no relevant changes in metabolic activity was observed at any concentration. Additionally, qualitative image analysis showed normal cell morphology on control surfaces but almost no cell adhesion to LIS modified titanium (Appendix Figure A7). Taking both these results and the lower bacterial membrane damage (Fig. 2D–G) into account, PDMS100 was ultimately selected for LIS integration into the INTER$_b$ACT model (Fig. 3C). Following the established protocol [21], pre-colonized control and partially LIS functionalized titanium implants were integrated into the fibroblast-containing collagen hydrogel prior to epithelial cell seeding. Tissue reaction with regard to cytokine secretion and tissue morphology was then analyzed after epithelial stratification at the air-liquid interface (in total 20 days of LIS-cell contact). The concentrations of the cytokines and chemokines IL-1β, TNF-α, CCL20 and IL-6 in the medium were quantified by ELISA and did not show any differences between unmodified controls and LIS functionalized samples (Fig. 3D). Histological grindings of Elastica van Gieson stained tissues showed a thin and intact multilayered epithelium on top of the connective tissue for both sample types (Fig. 3D). The organotypic mucosa was also fully attached to the inserted implant material. As expected, for control samples, a colonization of the supra-mucosal implant areas by the epithelium could be observed (Fig. 3D, arrow), which could not be detected for PDMS100-infused samples.

3.4. Repellent properties of silicone-infused titanium at the implant material-tissue-biofilm interface

After successful model setup with intact soft tissue site-to-site to the LIS functionalization, the INTER$_b$ACT model was subjected to co-culture with an oral multispecies biofilm following the established protocol (Fig. 4A) [18]. Afterwards, tissue reaction and titanium colonization were analyzed by ELISAs for secreted cytokines and chemokines, histology for tissue morphology, and confocal microscopy with digital image analysis for bacteria and cell attachment. As shown in Fig. 4B, concentrations of IL-1β, TNF-α, CCL20 and IL-6 in the supernatant did again not differ between control and PDMS100 coated samples. Interestingly, when comparing cytokine and chemokine levels after coculture with those of integration, a significant increase of IL-1β, as well as significant decreases of both CCL20 and IL-6 were observed (Appendix Figure A2B). Tissue morphology displayed by histological Elastica van Gieson stained grindings showed a loosened and slightly thickened epithelium for both groups (Fig. 4C); however, the connective tissues were still intact, and the organotypic mucosae were still fully attached to the inserted implant material below the functionalization. Regarding implant material colonization, differences between the LIS and the control group could already be seen by the representative CLSM images (Fig. 4D and E). For the control group, green fluorescence was detected at the supra-mucosal material areas on top of the bright fluorescent epithelial belt.Silicone-coated samples appeared darker and showed some lubricant reflection. This qualitative observation was supported by digital image analysis of the implant sides, which found 75 % less volume on the LIS functionalized samples (Fig. 4F). The composition of this volume was further dissected by neural network image analysis and revealed that the majority of the surface of the control group (approx.

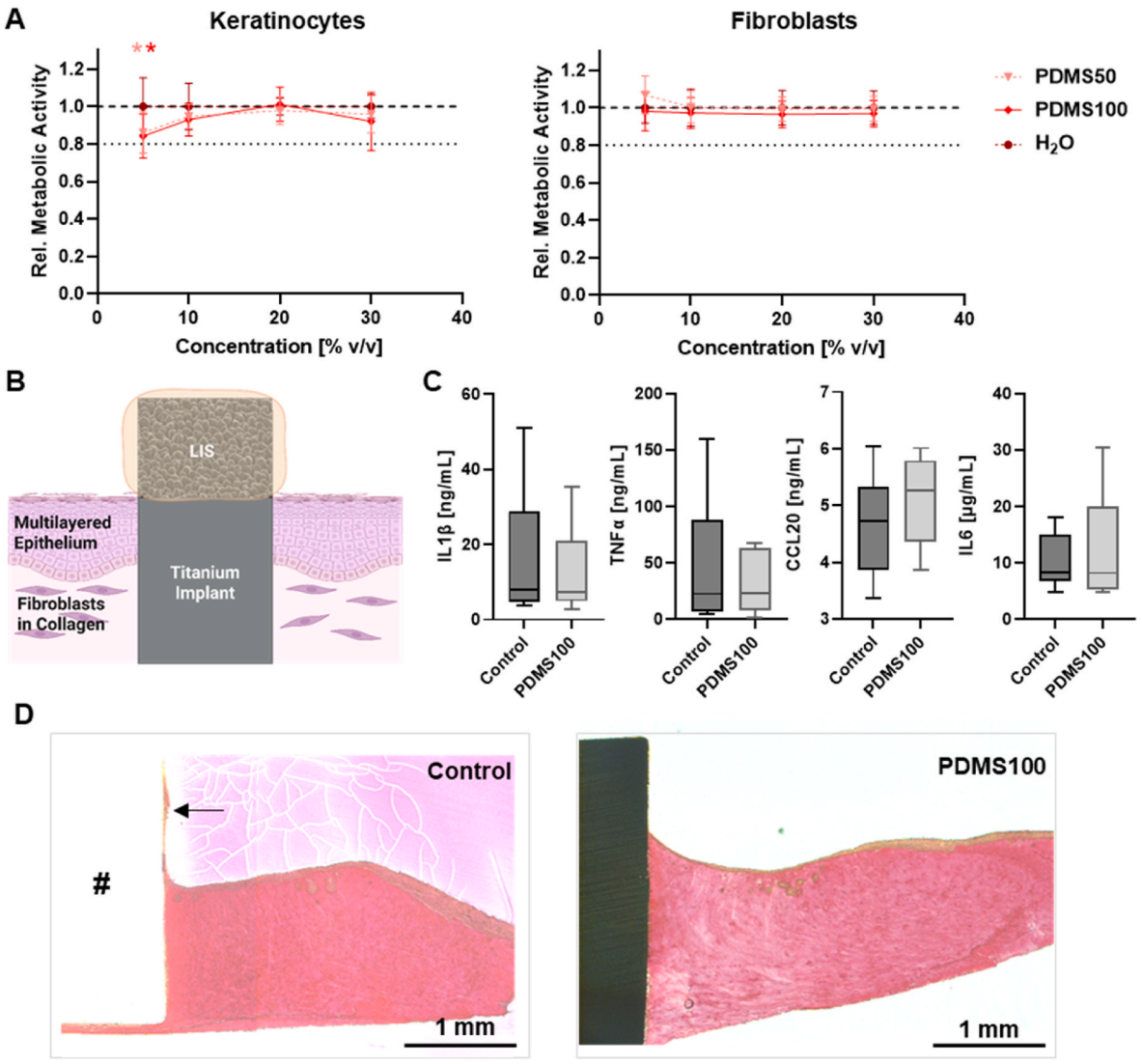

Fig. 3. *In vitro* tissue integration in direct contact to silicone-infused spike-structured titanium. (A) Mean ± standard deviation of metabolic activity of oral keratinocytes and human gingival fibroblasts incubated for 24 h with different concentrations of LIS components. * indicates statistically significant differences to the water control of the respective concentration with $p \leq 0.05$. Dotted lines indicate cytotoxic threshold. (B) Schematics of LIS functionalized titanium integrated into the INTER$_b$ACT model. (C) Tukey boxplots of different cytokines and chemokines quantified from the supernatant after model assembly and stratification. (D) Representative Elastica van Gieson stained histological grindings of the INTER$_b$ACT model. # indicates an implant that was lost during preparation. Arrow indicates epithelial growth on the implant.

100 %) was covered with human cells, and only a very small fraction was actually bacteria (Fig. 4G). A significant reduction in cell surface coverage to approx. 50 % could be observed on PDMS100 coated samples, which, however, did not lead to a change in cell/bacteria distribution. The viability of cells and bacteria did not differ between both groups and showed approx. 40 % viability on control and PDMS100 coated surfaces (Fig. 4H).

4. Discussion

To prevent the development of peri-implant infections caused by highly tolerant oral biofilms, antiadhesive surface modifications that inhibit the initial bacterial surface attachment (but at the same time do not impair the peri-implant tissue) are a vitally needed technological advancement. Within the present study, liquid-infused titanium surfaces that are suitable for application on medical-devices in terms of biocompatibility have been developed that showed statistically significant oral multispecies biofilm reduction under *in vitro* conditions mimicking the complex 3D environment of dental implants. Additionally, we have demonstrated that these antiadhesive properties neither affect the adjacent artificial oral mucosa nor increase the secretion of pro-inflammatory cytokines.

Biocompatible titanium LIS were generated by combining surface structuring, optional functionalization, and lubricant coating. Previous titanium LIS have been generated by combining spike-structured surfaces with Antispread fluoropolymer functionalization and GPL perfluoropolyether coating [8]. Even though this combination is not applicable to medical devices, functional LIS could nevertheless be generated via this method for use as control surfaces in this study. To develop medical device-compatible titanium LIS, spike surface structuring by ultra-short pulsed laser ablation was maintained. Since the self-assembled structure is generated by direct titanium sublimation through the laser pulses without any chemical modification of the remaining material, it is a solely physical process that conforms with medical device approval [24]. Additionally, a ripple structure of smaller dimension created with the same method was tested in combination with the lower viscous lubricants PFPHP and PFD. As has previously been shown for lower viscous perfluoropolyether [8], it was not able to

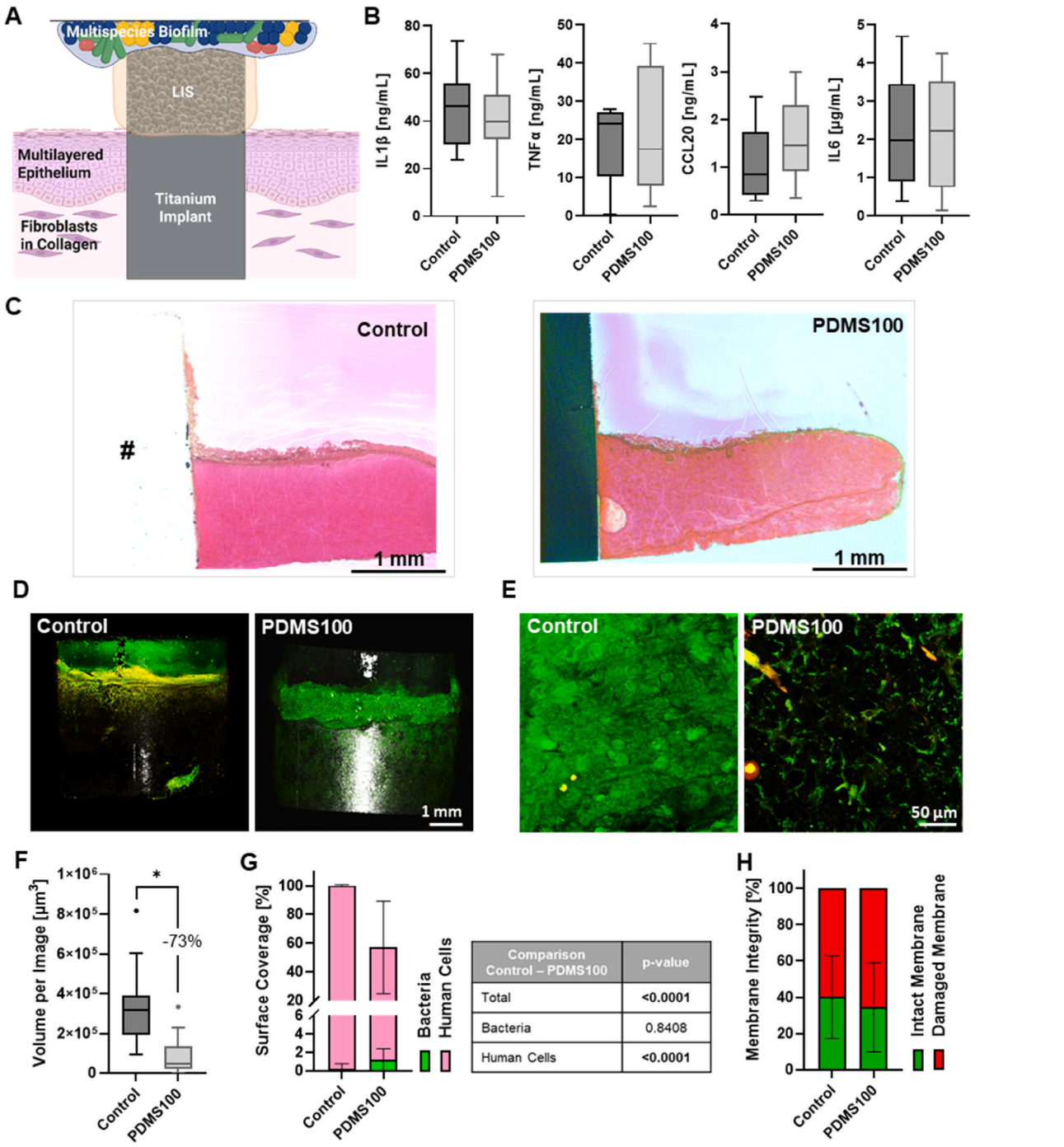

Comparison Control – PDMS100	p-value
Total	<0.0001
Bacteria	0.8408
Human Cells	<0.0001

Fig. 4. Influence of silicone-infused titanium on the implant-tissue-biofilm interaction *in vitro*. (A) Schematics of LIS functionalized titanium integrated into the INTER$_b$ACT model in coculture with an oral multispecies biofilm. (B) Tukey boxplots of different cytokines quantified from the supernatant after 48 h coculture. (C) Representative Elastica van Gieson stained histological grindings of the INTER$_b$ACT model after 48 h coculture. # indicates an implant that was lost during preparation. (D) Representative CLSM images (maximum projection presentation) of implants after removal from the cocultured INTER$_b$ACT model and (E) images of the supra-mucosal implant side used for quantification. Cells and bacteria with intact membrane are shown in green. Cells and bacteria with damaged membrane are shown in yellow/red. (F) Tukey boxplots of biofilm volumes per image of 295 × 295 µm^2 as well as mean ± standard deviation of (G) bacteria and human cell surface coverage with p-values from comparing control and LIS, and (H) biofilm membrane integrity of the different samples after 24 h of coculture quantified on the supra-mucosal implant sides. * indicate statistically significant differences with $p \leq 0.05$.

sufficiently trap the lubricants – probably due to a too low number of retention sites.

The first medical-grade lubricant tested was PFPHP, which is a hydrophobic and chemically inert perfluorinated cyclic hydrocarbon that is commonly used as vitreous replacement for the treatment of large retinal tears in ophthalmic surgery as well as blood substitute [25]. Due to similarities in its chemical structure compared to GPL, it was combined with Antispread functionalization. This led to LIS formation on spike structures according to the low contact angle hysteresis. However, after 1 h incubation in air, the lubricant thickness was already reduced by 50 %, which could be attributed to the substance's volatility [15]. Moreover, when incubating in liquid, no lubricant coating could be measured at all – indicating PFPHPs full detachment from the titanium surface. In contrast to PFPHP-infused PTFE membranes, where the

lubricant remained stable in liquid [15,26], the capillary trapping forces on modified titanium seems to be lower than the tendency to reduce surface tension by sphere formation and detachment. This rendered PFPHP unsuitable for LIS formation.

The next lubricant tested was PFD, which is likewise a hydrophobic and inert perfluorinated cyclic hydrocarbon used for the management of retinal tears and as blood substitute [25]. According to the low contact angle hysteresis, a LIS coating on spike structures functionalized with Antispread could be formed. However, the coating entirely evaporated after 1 h at ambient air due to its high volatility. Even though the lubricant was more stable when incubated in liquid, this characteristic likewise excluded PFD as reliable coating for titanium LIS.

Aside from the perfluorinated lubricants, two silicone oils of different viscosities (50 cSt and 100 cSt) were also tested since they are two of the most common medical-grade lubricants for LIS generation [25]. In contrast to the previous lubricants, the hydrophobic and inert aliphatic hydrocarbons were not paired with Antispread functionalization, but rather with MTMS and DTMS, due to their similar chemical structure in addition to unfunctionalized spike-structured titanium. Interestingly, according to contact angle hysteresis measurement, only PDMS coated on unfunctionalized titanium resulted in LIS formation. This is most probably due to the unfavorable changes in wettability by MTMS and DTMS functionalization – leading to hydrophilic surfaces that did not allow for a stable hydrophobic lubricant trapping in the hydrophilic environment. Even though both MTMS and DTMS are hydrophobic themselves, they probably covered the spike structure and by doing so reduced their natural super-hydrophobic properties. Nevertheless, the PDMS coatings on unfunctionalized titanium were found to be stable in air as well as in liquid. As the coating was quite thick compared to all other combinations under the current preparation method (drop coating with tilting to remove excess lubricant), a different procedure, like spin-coating, could be used for clinical application. In a previous study, this has led to coating thickness of approx. 100 μm only [8]. In addition, LIS also seem to find an equilibrium thickness of similar size when exposed to constant flow like in the oral cavity independently of the initial lubricant volume [9]. Even in this flow chamber setting, despite several high-velocity flushing steps and multiple observed air bubbles, the LIS remained stable over the entire 7 days of the experiment. This is in line with results of previous, non-biocompatible LIS, which were stable over the entirety of a 14-day-long experiment [8]. Therefore, PDMS coating on unfunctionalized titanium was selected as most promising titanium LIS for further biological evaluation. Nevertheless, it has to be taken into account that more elaborated stability tests are required before future application in the oral cavity. These should not only consider shear forces exhibited by salivary flow that can be replicated in *in vitro* experiments, but also potential mechanical forces exerted by the tongue or daily oral hygiene *in vivo*.

Before assessing biofilm-repellency, the silicone oils (along with Antispread and GPL of the control surfaces) were also tested for any toxic effect towards *S. oralis*. This bacterium was selected as a model organism for toxicity testing and the initial biofilm test since it is a major component of commensal biofilms and one of the first species which typically adheres to surfaces within the oral cavity [27]. Since the oral cavity actually accommodates several hundred bacterial species that grow in the presence of constant shear forces by salivation, however, the HOBIC model was used for biofilm testing. Within this established flow chamber system, a four-species biofilm of commensal composition was grown, with featuring high amounts of early colonizers *S. oralis*, *A. naeslundii* and *V. dispar* and comparatively low amounts of the late-colonizing oral pathogen *P. gingivalis* [17]. Especially at lower concentrations, bacterial growth and metabolic activity were not reduced by the presence of PDMS as well as Antispread and GPL. Thus, as might be expected from a product used for biomedical applications, PDMS showed no strong bacteriotoxic effect even though the increased metabolic activity at higher concentrations can be interpreted as inducing certain stress reactions [28,29]. This result is in line with biofilm viability analysis of both statically grown *S. oralis* monospecies biofilms and the oral multispecies biofilm grown in the HOBIC model, where only a modest increase in the amount of cells with damaged membranes was observed. The stronger increase of cells with damaged membranes on GPL-LIS was also observed in our previous study [8]. In contrast to the low effect on bacterial viability, biofilm volume was statistical significantly reduced on PDMS-LIS surfaces under both cultivation conditions. This effect was even maintained when incubating PDMS100-LIS with *S. oralis* for 7 days, indicating that the surface will not be easily overcome by sheer amounts of bacteria and a longer window of opportunity for colonization. PDMS100-LIS also retained their characteristic water contact angle and contact angle hysteresis when incubated in ambient air at 37 °C for 7 days, which, combined with the previous 7-day-experiment, indicates stability in both, aqueous media and air, being the precondition for prolonged biofilm-repellency. The effect of significantly reducing biofilm volume without affecting bacterial viability is characteristic for liquid-infused surfaces, and can be attributed to reduced bacterial adhesion forces on the coating lubricant compared to the solid control [9]; as a result, adhering biofilm can easily be removed by increased shear forces, like pipetting or higher flow velocities in the HOBIC model. The biofilm does not react to these lower adhesion forces on a metabolic level as previously analyzed by RNA sequencing, which drastically reduces the risk of resistance development [9]. The lower repellence of the multispecies biofilm compared to the *S. oralis* monospecies biofilm has already been described for GPL-LIS [9]. It is most probably due to supportive inter-species interactions that increase surface persistence. Furthermore, the HOBIC model also represents a "worst case" scenario, with a large volume of highly concentrated bacteria. When considering also the relatively low flow velocities (maximum 1 mL/min of laminar flow vs. up to 7 mL/min turbulent flow in the oral cavity [30]), maintaining more than 50 % biofilm reduction even under these conditions points towards the effectiveness of the LIS functionalization and the necessity for further analysis under *in vivo* conditions. When considering multispecies biofilms, varying effects on different species could be a concern, especially in the case of pathogenic late colonizers, like *P. gingivalis*. While qualitatively comparing bacteria shapes and biofilm structures in CLSM images of live/dead-stained biofilms on titanium and PDMS100-LIS from the HOBIC model, no significant differences in species distribution and biofilm structures could be found. This indicates similar biofilm compositions and, thus, no species-specific effects, which, however, needs to be analyzed with further, more detailed methods. Regarding *P. gingivalis*, it has to be mentioned that it, under the given cultivation conditions, only makes up a very small portion of the biofilm [17]. Taking into account the comparably low adhesion forces of *P. gingivalis* [19] and its specialty of adhering to other bacteria instead of substrates, we consider a selective increase of *P. gingivalis* as very unlikely.

In parallel to the LIS component's toxicity testing vis-á-vis bacteria, cytotoxicity towards oral keratinocytes and gingival fibroblasts was tested. No reduction in cellular metabolic activity below the cytotoxic threshold of 80 % was observed, which we attribute to component's chemical inertness and aligns with the medical use of PDMS. To analyze the biocompatibility of silicone-infused titanium in a clinically relevant *in vitro* setting, the INTER$_b$ACT model was then used. This 3D implant-mucosa-biofilm co-culture model consists of a multilayered artificial mucosa with an integrated titanium implant that can be challenged with the already described oral multispecies biofilm [18]. It provides an *in vitro* replication of the clinical soft tissue contact between all three components, and is therefore very well suited to test how biomaterials could potentially influence or impact this interaction. Since the PDMS-LIS (like most LIS) exhibited antiadhesive properties towards human cells [13], only the supra-mucosal part was modified before insertion into the model – simulating a supra-mucosally placed implant abutment. Therefore, the outcomes from the INTER$_b$ACT model result from a side-to-side lubricant contact to the stratified epithelium, but not

the connective tissue, similar to the clinical abutment situation. As indicated by unchanged secretion of cytokines and intact histological sections, biocompatible LIS modified titanium implants did not lead to any observable differences in this interaction when compared to unmodified titanium. The tested pro-inflammatory cytokines were selected since IL-1β, TNFα, and CCL20 have all previously been shown to be responsive within the INTER$_b$ACT model, and IL-1β and IL-6 are both involved in foreign body reaction [18,31]. The missing additional pro-inflammatory reaction towards the LIS modified titanium is in line with an *in vivo* investigation of subcutaneously placed LIS on polytetrafluoroethylenes [15]. This underscores the biocompatibility of the developed surface modification, and also the relevance and importance of the INTER$_b$ACT model. Interestingly, the histological sections showed a spreading of the epithelium to the supra-mucosal parts of the implants for the unmodified controls but not the LIS modified titanium. This should again be attributed to the antiadhesive LIS surface, and ought to be taken into account when assessing the appropriateness of this material for potential future medical applications.

Finally, the INTER$_b$ACT model containing the PDSM-LIS modified implant was co-cultured with the oral multispecies biofilm and analyzed for inflammatory reaction, tissue morphology, and implant surface colonization. Before co-cultivation, the partly structured, tissue-integrated implant material was re-coated with the lubricant. The following results, thus, also support the observation that LIS can be refilled (e.g., in the case of accessible implant parts like the abutment) and maintain their functionality. This is further important when considering potential mechanical lubricant removal due to mechanical shear forces in the oral cavity. Nevertheless, to reduce the need for re-coating the structured surface, future studies could also explore a (partial) covalent binding of silicone polymers onto the surface.

It has previously been shown that IL-1β, TNFα, and CCL20 – but not IL-6 – increased after prolonged bacterial co-culture compared to sterile conditions [18]. This was attributed to an increasing disruption of the host-microbiome homeostasis, which is clinically associated with infection progression. When comparing the cytokine secretion of sterile integration and biofilm co-culture of this study, it was observed that the levels of all but IL-1β decreased independently of the implant used. However, this could also be due to the entirely different cultivation conditions which make a direct comparison impossible. The secreted pro-inflammatory cytokines IL-1β, TNFα, CCL20 and IL-6 did not show any differences between modified and control implant under co-culture conditions. The antiadhesive LIS implant modification could therefore not inhibit the bacteria-driven pro-inflammatory conditions within the model. This most likely stems from the local effect of the LIS modification: even though it effectively reduces adhesion, the surface has no antibacterial properties and does not release any antibacterial components [9]. Tissue and biofilm not only have direct contact via the inserted implant within the model, but also through the shared liquid environment. This allows for an interaction via substance diffusion which could induce a pro-inflammatory reaction. This hypothesis is further supported by the histological results: independently of the inserted implant, both epitheliums showed a certain disintegration and exhibited a rather loosened structure. It has already been shown that this is not a direct disruption by bacterial cells, but rather part of the tissue's pro-inflammatory reaction to allow immune cells (such as neutrophiles) to migrate towards the bacteria under clinical conditions [21].

In contrast to the unchanged pro-inflammatory tissue reaction, quantification of implant surface colonization clearly showed reduced adhesion on the LIS titanium. Interestingly, the overall effect was larger in the INTER$_b$ACT model containing human cells and the multispecies biofilm than in the HOBIC model containing the multispecies biofilm only. A supportive effect for antibacterial substances by bacterial-cell interaction has already been shown for silver-gold nanoparticles in a more straight forward co-culture setup, and this has been attributed to the simultaneous cell self-defense [32]. In addition, we note that the "biofilm" on the implant surfaces of the INTER$_b$ACT model was observed to mainly consist of human cells, which are probably more susceptible to the antiadhesive modification. The pure antiadhesive nature of surface's effect was once again confirmed by membrane integrity-based viability staining, which did not differ between LIS and control group. We believe that the relatively larger amount of damaged membranes observed in this model compared to the HOBIC model should be attributed to the high amount of human cells implicated herein. The applied fluorescence staining kit is specifically dedicated to bacterial membrane properties (manufacturer's protocol, LIVE/DEAD®*Bac*Light™ Bacterial Viability Kit). When using it for human cells, both dyes are able to unspecifically enter the nucleus causing an increase in red fluorescence. Interestingly, even though the cell surface coverage on the LIS modified implants was significantly reduced, this did not lead to a significant increase of adhering bacteria, which accounted for only 1 % surface coverage. According to the "race for the surface" theory, biomaterials that are not sealed by human tissue are prone to bacterial attachment [33,34]. However, even though the LIS titanium were not covered by human cells, bacteria were not able to colonize the surface. This observation strengthens the antiadhesive effect of this modification that persists even in the 3D setup containing implant, tissue, and bacterial biofilm.

5. Conclusion

Implant surface modifications that reliably reduce bacterial colonization hold tremendous promise as a key element in the ongoing quest to reduce the rate of peri-implant infections. Through the present study, we have identified a stable, medical device-suitable and biofilm-reducing LIS modification that is based on laser-structured titanium surfaces coated with silicone oil. This surface coating was able to statistical significantly reduce biofilm accumulation under physiologically relevant conditions – including an oral multispecies biofilm grown under constant flow within the HOBIC model, as well as at the interface of human tissue, biofilm, and implant within the context of the INTER$_b$ACT model. In parallel, the titanium LIS was confirmed not to be cytotoxic – not altering the adjacent soft tissue or elevating pro-inflammatory cytokine secretion. These characteristics make the titanium LIS highly promising for further analysis in the context of targeted pre-clinical clinical studies. To overcome the limitations of the current *in vitro* analyses, such future studies should seek to assess these coating's stability and biofilm repellency properties under the type of shear forces which arise for dental implant abutments directly at the oral transmucosal implant site *in vivo*. The influence of the coating on different bacterial species and composition of multispecies biofilms should also be investigated. Additionally, such analyses should also seek to verify and expand our preliminary understanding concerning the *in vitro* immune reaction and biocompatibility results, including assessment of the full immune system and all systemic effects on an entire body. However, when these pre-clinical studies lead to satisfactory results, the biocompatible titanium LIS developed and characterized in this study possess high potential to help contribute to the future prevention of peri-implant infections.

CRediT authorship contribution statement

Katharina Doll-Nikutta: Writing – original draft, Methodology, Investigation, Funding acquisition, Data curation, Conceptualization. **Carina Mikolai:** Writing – original draft, Methodology, Investigation, Data curation, Conceptualization. **Nils Heine:** Writing – original draft, Investigation, Data curation. **Kestutis Kurselis:** Writing – review & editing, Methodology, Investigation. **Elena Fadeeva:** Writing – review & editing, Methodology, Investigation. **Nicolas Debener:** Writing – review & editing, Methodology, Investigation. **Beate Legutko:** Writing – review & editing, Investigation. **Charlotte Kreuzkamp:** Writing – review & editing, Methodology, Investigation. **Vannila Prasanthan:** Writing – review & editing, Supervision. **Janina Bahnemann:** Writing – review & editing, Supervision, Funding acquisition. **Boris N. Chichkov:**

Writing – review & editing, Supervision, Funding acquisition, Conceptualization. **Meike Stiesch:** Writing – review & editing, Supervision, Funding acquisition, Conceptualization.

Data statement

The data are available upon request from the corresponding author.

Ethics approval and consent to participate

No ethical approval and informed consent were necessary for this *in vitro* study.

Declaration of competing interest

All authors declare no conflict of interest.

Acknowledgements

The work was funded by the Deutsche Forschungsgemeinschaft (DFG, German Research Foundation) under the Collaborative Research Center SFB/TRR-298-SIIRI – Project ID 426335750 and by the Deutsche Gesellschaft für Prothetische Zahnmedizin und Biomaterialien e.V. (DGPro, German Society for Prosthetic Dentistry and Biomaterials). The authors would like to thank Andreas Winkel for providing graphics created in BioRender and Henning Hartwig and Hanna Lena Thoms for excellent technical assistance.

Appendix A. Supplementary data

Supplementary data to this article can be found online at https://doi.org/10.1016/j.bioactmat.2025.07.048.

References

[1] Deutsche Gesellschaft Fuer Implantologie Im Zahn-, Mund- Und Kieferbereich E. V. Presse-Information 30.11.2018, 2018.
[2] H. Dreyer, J. Grischke, C. Tiede, J. Eberhard, A. Schweitzer, S.E. Toikkanen, S. Glöckner, G. Krause, M. Stiesch, Epidemiology and risk factors of peri-implantitis: a systematic review, J. Periodontal. Res. 53 (2018) 657–681.
[3] H. Flemming, J. Wingender, U. Szewzyk, P. Steinberg, S.A. Rice, S. Kjelleberg, Biofilms: an emergent form of bacterial life, Nat. Rev. Microbiol. 14 (2016) 563–575.
[4] P.E. Kolenbrander, R.J. Palmer Jr., S. Periasamy, N.S. Jakubovics, Oral multispecies biofilm development and the key role of cell-cell distance, Nat. Rev. Microbiol. 8 (2010) 471–480.
[5] D. Davies, Understanding biofilm resistance to antibacterial agents, Nat. Rev. Drug Discov. 2 (2003) 114–122.
[6] G. Hajishengallis, Periodontitis: from microbial immune subversion to systemic inflammation, Nat. Rev. Immunol. 15 (2015) 30–44.
[7] T.S. Wong, S.H. Kang, S.K. Tang, E.J. Smythe, B.D. Hatton, A. Grinthal, J. Aizenberg, Bioinspired self-repairing slippery surfaces with pressure-stable omniphobicity, Nature 477 (2011) 443–447.
[8] K. Doll, E. Fadeeva, J. Schaeske, T. Ehmke, A. Winkel, A. Heisterkamp, B. N. Chichkov, M. Stiesch, N.S. Stumpp, Development of laser-structured liquid-infused titanium with strong biofilm-repellent properties, ACS Appl. Mater. Interfaces 9 (2017) 9359–9368.
[9] K. Doll, I. Yang, E. Fadeeva, N. Kommerein, S.P. Szafranski, G. Bei der Wieden, A. Greuling, A. Winkel, B.N. Chichkov, N.S. Stumpp, M. Stiesch, Liquid-infused structured titanium surfaces: antiadhesive mechanism to repel Streptococcus oralis biofilms, ACS Appl. Mater. Interfaces 11 (2019) 23026–23038.
[10] M. Villegas, Y. Zhang, M. Badv, C. Alonso-Cantu, D. Wilson, Z. Hosseinidoust, T. F. Didar, Enhancing osseointegration and mitigating bacterial biofilms on medical-grade titanium with chitosan-conjugated liquid-infused coatings, Sci. Rep. 12 (2022) 5380–5384.
[11] Y. Li, Y. Zhou, J. Lin, H. Liu, X. Liu, Antifouling slippery surface with enhanced stability for marine applications, Materials (Basel) 17 (2024) 5598, https://doi.org/10.3390/ma17225598.
[12] Y. Yang, Q. Zhu, L. Xu, X. Zhang, Bioinspired liquid-infused surface for biomedical and biosensing applications, Front. Bioeng. Biotechnol. 10 (2022) 1032640.
[13] C. Howell, A. Grinthal, S. Sunny, M. Aizenberg, J. Aizenberg, Designing liquid-infused surfaces for medical applications: a review, Adv. Mater. 30 (2018) e1802724.
[14] D.C. Leslie, A. Waterhouse, J.B. Berthet, T.M. Valentin, A.L. Watters, A. Jain, P. Kim, B.D. Hatton, A. Nedder, K. Donovan, E.H. Super, C. Howell, C.P. Johnson, T.L. Vu, D.E. Bolgen, S. Rifai, A.R. Hansen, M. Aizenberg, M. Super, J. Aizenberg, D.E. Ingber, A bioinspired omniphobic surface coating on medical devices prevents thrombosis and biofouling, Nat. Biotechnol. 32 (2014) 1134–1140.
[15] J. Chen, C. Howell, C.A. Haller, M.S. Patel, P. Ayala, K.A. Moravec, E. Dai, L. Liu, I. Sotiri, M. Aizenberg, J. Aizenberg, E.L. Chaikof, An immobilized liquid interface prevents device associated bacterial infection in vivo, Biomaterials 113 (2017) 80–92.
[16] J. Yin, M.L. Mei, Q. Li, R. Xia, Z. Zhang, C.H. Chu, Self-cleaning and antibiofouling enamel surface by slippery liquid-infused technique, Sci. Rep. 6 (2016) 25924.
[17] N. Kommerein, K. Doll, N.S. Stumpp, M. Stiesch, Development and characterization of an oral multispecies biofilm implant flow chamber model, PLoS One 13 (2018) e0196967.
[18] C. Mikolai, N. Kommerein, A. Ingendoh-Tsakmakidis, A. Winkel, C. Falk, M. Stiesch, Early host microbe interaction in a periimplant oral mucosa-biofilm model, Cell. Microbiol. (2020) e13209.
[19] K. Doll-Nikutta, A. Winkel, I. Yang, A.J. Grote, N. Meier, M. Habib, H. Menzel, P. Behrens, M. Stiesch, Adhesion forces of oral bacteria to titanium and the correlation with biophysical cellular characteristics, Bioengineering (Basel) 9 (2022) 567, https://doi.org/10.3390/bioengineering9100567.
[20] M.A. Dickson, W.C. Hahn, Y. Ino, V. Ronfard, J.Y. Wu, R.A. Weinberg, D.N. Louis, F.P. Li, J.G. Rheinwald, Human keratinocytes that express hTERT and also bypass a p16(INK4a)-enforced mechanism that limits life span become immortal yet retain normal growth and differentiation characteristics, Mol. Cell Biol. 20 (2000) 1436–1447.
[21] A. Ingendoh-Tsakmakidis, C. Mikolai, A. Winkel, S.P. Szafranski, C.S. Falk, A. Rossi, H. Walles, M. Stiesch, Commensal and pathogenic biofilms differently modulate peri-implant oral mucosa in an organotypic model, Cell. Microbiol. 21 (2019) e13078.
[22] W. Rasband, Imagej - Image Processing and Analysis in Java, vol. 1, 2011, p. 48v.
[23] M. Pachitariu, C. Stringer, Cellpose 2.0: how to train your own model, Nat. Methods 19 (2022) 1634–1641.
[24] Y.L. Yao, H.Q. Chen, W.W. Zhang, Time scale effects in laser material removal: a review, Int. J. Adv. Manuf. Technol. 26 (2005) 598–608.
[25] S. Peppou-Chapman, J.K. Hong, A. Waterhouse, C. Neto, Life and death of liquid-infused surfaces: a review on the choice, analysis and fate of the infused liquid layer, Chem. Soc. Rev. 49 (2020) 3688–3715.
[26] M. Badv, C. Alonso-Cantu, A. Shakeri, Z. Hosseinidoust, J.I. Weitz, T.F. Didar, Biofunctional lubricant-infused vascular grafts functionalized with silanized bio-inks suppress thrombin generation and promote endothelialization, ACS Biomater. Sci. Eng. 5 (2019) 6485–6496.
[27] A.P.V. Colombo, A.C.R. Tanner, The role of bacterial biofilms in dental caries and periodontal and peri-implant diseases: a historical perspective, J. Dent. Res. 98 (2019) 373–385.
[28] N. Kommerein, N. Vierengel, J. Gross, T. Opatz, B. Al-Nawas, L.K. Muller-Heupt, Antiplanktonic and antibiofilm activity of Rheum palmatum against Streptococcus oralis and Porphyromonas gingivalis, Microorganisms 10 (2022) 965, https://doi.org/10.3390/microorganisms10050965.
[29] N. Kommerein, A.J. Weigel, M. Stiesch, K. Doll, Plant-based oral care product exhibits antibacterial effects on different stages of oral multispecies biofilm development in vitro, BMC Oral Health 21 (2021) 170–174.
[30] S.P. Humphrey, R.T. Williamson, A review of saliva: normal composition, flow, and function, J. Prosthet. Dent 85 (2001) 162–169.
[31] J.M. Anderson, A. Rodriguez, D.T. Chang, Foreign body reaction to biomaterials, Semin. Immunol. 20 (2008) 86–100.
[32] K. Doll-Nikutta, N. Heine, M. Kheirmand-Parizi, F. Stein, J. Ulrich, C. Rehbock, A. Winkel, S. Barcikowski, M. Stiesch, Bacteria-epithelial cell interaction influences cytotoxicity and antibacterial effect of silver-gold alloy nanoparticles on a species-specific level, ChemNanoMat 10 (2023) e2023004.
[33] A.G. Gristina, Biomaterial-centered infection: microbial adhesion versus tissue integration, Science 237 (1987) 1588–1595.
[34] B. Zhao, H.C. van der Mei, G. Subbiahdoss, J. de Vries, M. Rustema-Abbing, R. Kuijer, H.J. Busscher, Y. Ren, Soft tissue integration versus early biofilm formation on different dental implant materials, Dent. Mater. 30 (2014) 716–727.